

---

1      **Underestimation of Anthropogenic Organosulfates in Atmospheric**  
2      **Aerosols in Urban Regions**

3      *Yanting Qiu<sup>1#</sup>, Junrui Wang<sup>1#</sup>, Tao Qiu<sup>2</sup>, Jiajie Li<sup>3</sup>, Yanxin Bai<sup>4</sup>, Teng Liu<sup>1</sup>, Ruiqi Man<sup>1</sup>,*  
4      *Taomou Zong<sup>1</sup>, Wenxu Fang<sup>1</sup>, Jiawei Yang<sup>1</sup>, Yu Xie<sup>1</sup>, Zeyu Feng<sup>1</sup>, Chenhui Li<sup>3</sup>, Ying Wei<sup>3</sup>,*  
5      *Kai Bi<sup>5</sup>, Dapeng Liang<sup>2</sup>, Ziqi Gao<sup>6</sup>, Zhijun Wu<sup>1,7,\*</sup>, Yuchen Wang<sup>4,\*</sup>, Min Hu<sup>1</sup>*

6      <sup>1</sup> State Key Laboratory of Regional Environment and Sustainability, International Joint  
7      Research Center for Atmospheric Research (IJRC), College of Environmental Sciences  
8      and Engineering, Peking University, Beijing, China

9      <sup>2</sup> Key Lab of Groundwater Resources and Environment of the Ministry of Education,  
10     College of New Energy and Environment, Jilin University, Changchun, China

11     <sup>3</sup> College of Environment and Ecology, Laboratory of Compound Air Pollutions  
12     Identification and Control, Taiyuan University of Technology, Taiyuan, China

13     <sup>4</sup> College of Environmental Science and Engineering, Hunan University, Changsha,  
14     China

15     <sup>5</sup> Beijing Weather Modification Center, Beijing Meteorological Service, Beijing, China

16     <sup>6</sup> University of Virginia Environmental Institute, Charlottesville, United States

17     <sup>7</sup> Collaborative Innovation Center of Atmospheric Environment and Equipment  
18     Technology, Nanjing University of Information Science and Technology, Nanjing, China

19     #: Yanting Qiu and Junrui Wang contributed equally to this work

20     \*Correspondence Author:

21     Zhijun Wu (zhijunwu@pku.edu.cn) and Yuchen Wang (ywang@hnu.edu.cn)

22

---

23 **ABSTRACT**

24 Organosulfates (OSs) are important components of organic aerosols, which serve as  
25 critical tracers of secondary organic aerosols (SOA). However, molecular composition,  
26 ~~precursor OS correspondence~~ the relationship between OSs and their precursors, and  
27 formation driving factors of OSs at different atmospheric conditions have not been fully  
28 constrained. In this work, we integrated OS molecular composition, precursor-  
29 constrained positive matrix factorization (PMF) source apportionment, and OS-precursor  
30 correlation analysis to classify OS detected from PM<sub>2.5</sub> samples according to their volatile  
31 organic compounds (VOCs) precursors collected from three different cities (Beijing,  
32 Taiyuan, and Changsha) in China. This new approach enables the accurate classification  
33 of OSs from molecular perspective. Compared with conventional classification methods,  
34 we found the mass fraction of Aliphatic OSs (including nitrooxy OSs; NOSs) increased  
35 by 22.0%, 17.8%, and 10.3% in Beijing, Taiyuan, and Changsha, respectively,  
36 highlighting the underestimation of Aliphatic OSs in urban regions. The formation driving  
37 factors of Aliphatic OSs during the field campaign were further investigated. We found  
38 that elevated aerosol liquid water content promoted the formation of Aliphatic OSs only  
39 when aerosols transition from non-liquid state to liquid state. In addition, enhanced  
40 inorganic sulfate mass concentrations, and O<sub>x</sub> (O<sub>x</sub> = NO<sub>2</sub> + O<sub>3</sub>) concentrations, as well as  
41 decreased aerosol pH commonly facilitated the formation of Aliphatic OSs. These results  
42 reveal a significant underestimation of OSs derived from anthropogenic emissions in  
43 wintertime, particularly Aliphatic OSs, highlighting the need for a deeper understanding  
44 of SOA formation and composition in urban environments.

45 **KEY WORDS:** organosulfate; non-target analysis; high-resolution mass spectrometry;  
46 secondary organic aerosol; PMF source apportionment

---

## 48 1. Introduction

49 Due to the diversity of natural and anthropogenic emissions and the complexity of atmospheric  
50 chemistry, investigating the chemical characterization and formation mechanisms of secondary  
51 organic aerosols (SOA) remains challenging. Among SOA components, organosulfates (OSs) have  
52 emerged as key tracers (Brüggemann et al., 2020; Hoyle et al., 2011), as their formation is primarily  
53 governed by secondary atmospheric processes. Moreover, OS significantly influence the aerosol  
54 physicochemical properties, including acidity (Riva et al., 2019; Zhang et al., 2019), hygroscopicity  
55 (Estillore et al., 2016; Ohno et al., 2022; Hansen et al., 2015), and light-absorption properties (Fleming  
56 et al., 2019; Jiang et al., 2025). Therefore, a deeper understanding of OS abundance, sources, and  
57 formation drivers is crucial for elucidating SOA formation and its properties.

58 Quantifying OS abundance is critical to assess their contribution to SOA. However, this is  
59 difficult due to the large number and structural diversity of OSs molecules and the lack of authentic  
60 standards. Most studies quantify a few representative OSs using synthetic or surrogate standards  
61 (Wang et al., 2020; Wang et al., 2017; Huang et al., 2018b; He et al., 2022), while non-target analysis  
62 (NTA) with high-resolution mass spectrometry (HRMS) offers broader molecular characterization  
63 (Huang et al., 2023a; Wang et al., 2022b; Cai et al., 2020). Although NTA combined with surrogate  
64 standards allows molecular-level (semi-)quantification, overall OS mass concentration remain  
65 underestimated, and many OSs remain unidentified (Lukács et al., 2009; Cao et al., 2017; Tolocka and  
66 Turpin, 2012; Ma et al., 2025).

67 Classifying OS based on their precursors is a powerful approach for understanding OS formation  
68 from a mechanistic perspective. OSs from specific precursors generally share similar elemental  
69 compositions, with characteristic ranges of C atoms, double bond equivalents (DBE), and aromaticity  
70 equivalents (Xc). For example, isoprene-derived OSs typically contain 4–5 C atoms; monoterpene-  
71 and sesquiterpene-derived OSs usually have 9–10 and 14–15 C atoms, respectively (Lin et al., 2012;  
72 Riva et al., 2016c; Wang et al., 2019a; Surratt et al., 2008; Riva et al., 2015). An “OS precursor map,”  
73 correlating molecular weight and carbon number based on chamber studies, has been developed to  
74 classify OSs accordingly (Wang et al., 2019a). However, these approaches often oversimplify OS  
75 formation by relying solely on elemental composition, leaving many OSs without identified precursors.

76 The formation mechanisms of OS remain incompletely understood, though several driving  
77 factors have been identified through controlled chamber experiments and ambient observations. For  
78 instance, increased aerosol liquid water content (ALWC) enhances OS formation by promoting the  
79 uptake of gaseous precursors (Xu et al., 2021a; Wang et al., 2021b). Inorganic sulfate can also affect  
80 OS formation by acting as nucleophiles via epoxide pathway (Eddingsaas et al., 2010; Wang et al.,  
81 2020). However, meteorological conditions vary across cities, meaning the relative importance of  
82 these factors may differ by location. Thus, evaluating these formation drivers under diverse  
83 atmospheric conditions is essential. Identifying both common and region-specific drivers is key to a  
84 comprehensive understanding of OS formation mechanisms.

85 In this study, we employed NTA using ultra-high performance liquid chromatography (UHPLC)  
86 coupled with high-resolution mass spectrometry (HRMS) to characterize OS molecular composition  
87 in PM<sub>2.5</sub> samples from three cities. Identified OSs were classified by their VOCs precursors, including

88 aromatic, aliphatic, monoterpene, and sesquiterpene VOCs, via precursor-constrained positive matrix  
89 factorization (PMF). Mass concentrations were quantified or semi-quantified using authentic or  
90 surrogate standards. Additionally, spatial variations in OS mass concentrations and co-located  
91 environmentalenvironmental conditions factors were analyzed to distinguish both common and site-  
92 specific drivers of OS formation.

## 93 2. Methodology

### 94 2.1 Sampling and Filter Extraction

95 Field observations were conducted during winter (December 2023 to January 2024) at three urban  
96 sites in China: Beijing, Taiyuan, and Changsha. The site selection was based on contrasts in winter  
97 meteorological conditions and dominate PM<sub>2.5</sub> sources. For meteorological conditions, Beijing and  
98 Taiyuan represent northern Chinese cities with cold, dry conditions (low RH). In comparison,  
99 Changsha is characterized by relatively higher winter RH. In terms of PM<sub>2.5</sub> sources, Taiyuan is a  
100 traditional industrial and coal-mining base, Changsha's pollution profile is more influenced by traffic  
101 and domestic cooking emissions, whereas Beijing is characterized by a high mass fraction of  
102 secondary aerosols. This enables a comparative analysis of OS formation mechanisms under varied  
103 atmospheric conditions. In Beijing, PM<sub>2.5</sub> samples were collected at the Peking University Atmosphere  
104 Environment Monitoring Station (PKUERS; 40.00°N, 116.32°E), as detailed in previous studies  
105 (Wang et al., 2023a). Sampling in Taiyuan and Changsha took place on rooftops at the Taoyuan  
106 National Control Station for Ambient Air Quality (37.88°N, 112.55°E) and the Hunan Hybrid Rice  
107 Research Center (28.20°N, 113.09°E), respectively (see Figure S1).

108 Daily PM<sub>2.5</sub> samples were collected on quartz fiber filters ( $\phi = 47$  mm, Whatman Inc.) from 9:00  
109 to 8:00 local time the next day. All quartz fiber filters were pre-baked at 550 °C for 9 hours before  
110 sampling to remove the background organic matters. In Beijing and Taiyuan, RH-resolved sampling  
111 was performed using a home-made RH-resolved sampler, stratifying daily samples into low (RH  $\leq$   
112 40%), moderate (40%  $<$  RH  $\leq$  60%), and high (RH  $>$  60%) RH regimes with the sampling flow rate  
113 of 38 L/min. Due to persistently high RH in Changsha, a four-channel sampler (TH-16, Wuhan  
114 Tianhong Inc.) collected PM<sub>2.5</sub> samples without RH stratification with the flow rate of 16.7 L/min.  
115 Consequently, Beijing and Taiyuan collected one or more samples daily, whereas Changsha collected  
116 one sample per day. A total of 40, 64, and 30 samples were obtained from Beijing, Taiyuan, and  
117 Changsha, respectively. The samples were stored in a freezer at -18 °C immediately after collection.  
118 The maximum duration between the completion of sampling and the start of chemical analysis was  
119 approximately 40 days. Prior to analysis, all samples were equilibrated for 24 hours under controlled  
120 temperature (20  $\pm$  1 °C) and RH (40-45%) within a clean bench, in order to allow the filters to reach  
121 a stable, reproducible condition for subsequent handling and to minimize moisture condensation.  
122 Average daily PM<sub>2.5</sub> mass concentrations and RH during sampling are summarized in Table S1.

123 Sample extraction followed established protocols (Wang et al., 2020). Briefly, filters were  
124 ultrasonically extracted twice for 20 minutes. A total volume of 10 mL of LC-MS grade methanol  
125 (Merck Inc.) was used for each sample. All extracts were filtered through 0.22  $\mu$ m PTFE syringe filters,  
126 and evaporated under a gentle stream of high-purity N<sub>2</sub> ( $>99.99\%$ ). The dried extracts were then

127 redissolved in 2 mL of LC-MS grade methanol for analysis. This step was necessary to achieve  
128 sufficient sensitivity for the detection of OSs with low concentration.

129 During the campaign, gaseous pollutants (SO<sub>2</sub>, NO<sub>2</sub>, O<sub>3</sub>, CO) were monitored using automatic  
130 PM<sub>2.5</sub> and PM<sub>10</sub> mass concentrations were measured by tapered element oscillating  
131 microbalance (TEOM). Water-soluble ions (Na<sup>+</sup>, NH<sub>4</sub><sup>+</sup>, K<sup>+</sup>, Mg<sup>2+</sup>, Ca<sup>2+</sup>, Cl<sup>-</sup>, NO<sub>3</sub><sup>-</sup>, SO<sub>4</sub><sup>2-</sup>) were  
132 analyzed with the Monitor for AeRosols and Gases in ambient Air (MARGA) coupled with ion  
133 chromatography. Organic carbon (OC) and elemental carbon (EC) were quantified by online OC/EC  
134 analyzers or carbon aerosol speciation systems. Trace elements in PM<sub>2.5</sub> were determined by X-ray  
135 fluorescence spectrometry (XRF). Additionally, VOCs concentrations were measured using an online  
136 gas chromatography-mass spectrometry (GC-MS) system with a one-hour time resolution in Taiyuan  
137 and Changsha. Table S2 summarizes the monitoring instruments deployed at each site. All instruments  
138 were calibrated to ensure the reliability of the measurement data. Specifically, the online gas pollutants  
139 and particulate matter automatic analyzers underwent automatic zero/span checks every 24 hours at  
140 0:00 local time. For MARGA-ion chromatography, OC/EC analyzers, and XRF systems were  
141 calibrated weekly. The online GC-MS system was automatically calibrated every 24 hours using  
142 standard VOCs mixture.

## 143 2.2 Identification of Organosulfates

144 The molecular composition of PM<sub>2.5</sub> extracts was analyzed using an ultra-high performance  
145 liquid chromatography (UHPLC) system (Thermo Ultimate 3000, Thermo Scientific) coupled with an  
146 Orbitrap HRMS (Orbitrap Fusion, Thermo Scientific) equipped with an electrospray ionization (ESI)  
147 source operating in negative mode. Chromatographic separation was achieved on a reversed-phase  
148 Accucore C18 column (150 × 2.1 mm, 2.6 μm particle size, Thermo Scientific). For tandem MS  
149 acquisition, full MS scans (*m/z* 70–700) were collected at a resolving power of 120,000, followed by  
150 data-dependent MS/MS (ddMS<sup>2</sup>) scans (*m/z* 50–500) at 30,000 resolving power. Detailed UHPLC-  
151 HRMS<sup>2</sup> parameters are provided in Text S1.

152 NTA was performed using Compound Discoverer (CD) software (version 3.3, Thermo Scientific)  
153 to identify chromatographic peak features (workflow details in Table S3). Molecular formulas were  
154 assigned based on elemental combinations C<sub>c</sub>H<sub>h</sub>O<sub>o</sub>N<sub>n</sub>S<sub>s</sub> (c = 1–90, h = 1–200, o = 0–20, n = 0–1, s =  
155 0–1) within a mass tolerance of 0.005 Da with up to one <sup>13</sup>C isotope. Formulas with hydrogen-to-  
156 carbon (H/C) ratios outside 0.3–3.0 and oxygen-to-carbon (O/C) ratios beyond 0–3.0 were excluded  
157 to remove implausible assignments. We calculated the double bond equivalent (DBE) and aromatic  
158 index represented by X<sub>c</sub> based on assigned elemental combinations using eqs. (1) and (2), where *m*  
159 and *k* were the fractions of oxygen and sulfur atoms in the π-bond structures of a compound (both *m*  
160 and *k* were presumed to be 0.50 in this work (Yassine et al., 2014)).

161 DBE = c – 0.5h + 0.5n + 1 (1)

162 X<sub>c</sub> = (3 × (DBE – *m* × o – *k* × s) – 2) / (DBE – *m* × o – *k* × s) (if DBE < (*m* × o +  
163 *k* × s) or X<sub>c</sub> < 0, then X<sub>c</sub> was set to 0) (2)

164 In eq. (2), X<sub>c</sub> is an important indicator of whether aromatic rings exist in a molecule. Studies  
165 have proved that a molecule is considered aromatic if its X<sub>c</sub> value exceeds 2.50 (Ma et al., 2022;  
166 Yassine et al., 2014). OSs were selected based on compounds with O/S ≥ 4 and HSO<sub>4</sub><sup>-</sup> (*m/z* 96.96010)

167 fragments were observed in their corresponding  $MS^2$  spectra. Among them, if N number is 1, O/S  $\geq 7$ ,  
168 and their  $MS^2$  spectra showed  $ONO_2^-$  ( $m/z$  61.98837) fragment, these OSs were defined as nitrooxy  
169 OSs (NOSs). It should be noted that several CHOS (composed of C, H, O, and S atoms, hereinafter)  
170 and CHONS species were not determined as OSs due to their low-abundance and insufficient to trigger  
171 reliable data-dependent  $MS^2$  acquisition, which may lead to an underestimation of total OS mass  
172 concentration.

### 173 2.3 Classification and Quantification/Semi-quantification of Organosulfates

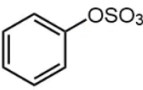
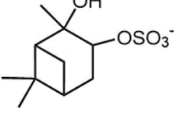
174 To ensure the reliability of quantitative analysis and source attribution, this study focuses on OS  
175 species with  $C \geq 8$ . The exclusion of smaller OSs ( $C \leq 7$ ) is based on challenges in their unambiguous  
176 identification, including co-elution with interfering compounds (Liu et al., 2024), and higher  
177 uncertainty in precursor assignment due to the lack of characteristic “tracer” molecules in laboratory  
178 experiments. Though re-~~dissolve~~ using pure methanol may not be the ideal solvent for  
179 retaining polar, early-eluting compounds on the reversed-phase column, it provided a consistent  
180 solvent for the analysis of the mid- and non-polar OS species ( $C \geq 8$ ) that are the focus of this study.

181 To classify the identified OSs, we employed and compared two distinct classification approaches.  
182 Firstly, a conventional classification approach relies primarily on precursor–product relationships  
183 established through controlled laboratory chamber experiments and field campaigns (Zhao et al., 2018;  
184 Wang et al., 2021a; Deng et al., 2021; Xu et al., 2021b; Mutzel et al., 2015; Brüggemann et al., 2020;  
185 Yang et al., 2024; Duporté et al., 2020; Huang et al., 2023b; Wang et al., 2022b; Riva et al., 2016a).  
186 Based on these established precursor–product relationships, detected OSs and NOSs were classified  
187 into four groups: Monoterpene OSs (including Monoterpene NOSs, hereinafter), Aliphatic OSs  
188 (including Aliphatic NOSs, hereinafter), Aromatic OSs (including Aromatic NOSs, hereinafter), and  
189 Sesquiterpene OSs (including Sesquiterpene NOSs, hereinafter) (see Table S4 for details). It is  
190 apparently that this approach has notable limitations when applied to detected OS in atmospheric  
191 aerosols. A substantial fraction of detected OSs does not match known laboratory tracers and are thus  
192 labeled Unknown OSs (including Unknown NOSs, hereinafter).

193 Synthetic  $\alpha$ -pinene OSs ( $C_{10}H_{17}O_5S^-$ ) and NOSs ( $C_{10}H_{16}NO_7S^-$ ) served for (semi-)quantifying  
194 Monoterpene and Sesquiterpene OSs. Their detailed synthesis procedure was described in previous  
195 study (Wang et al., 2019b). Potassium phenyl sulfate ( $C_6H_5O_4S^-$ ) and sodium octyl sulfate ( $C_8H_{17}O_4S^-$ )  
196 were used for Aromatic OSs and Aliphatic OSs due to lack of authentic standards (Yang et al., 2023;  
197 He et al., 2022; Staudt et al., 2014). Unknown OSs were semi-quantified by surrogates with similar  
198 retention times (RT) (Yang et al., 2023; Huang et al., 2023b). Table 1 lists the standards, retention  
199 times, and quantified categories. Unknown OSs were absent between 2.00–5.00 min and after 13.60  
200 min.

201 **Table 1** Chemical structure, UHPLC retention time, and quantified categories of standards used in  
202 the quantification/semi-quantification of OSs and NOSs

Formula (M-H)	$m/z$ ([M-H] $^-$ )	Chemical structure	UHPLC RT (min)	Quantified OSs categories
------------------	------------------------	--------------------	-------------------	---------------------------

<chem>C6H5O4S-</chem>	172.99140		0.92	Aromatic OSs, Unknown OSs (RT 0.50-2.00 min)
<chem>C8H17O4S-</chem>	209.08530		10.30	Aliphatic OSs, Unknown OSs (RT 10.00-13.60 min)
<chem>C10H17O5S-</chem>	249.08022		7.73	Monoterpene OSs, Sesquiterpene OSs, Unknown OSs (RT 5.00-10.00 min)
<chem>C10H16NO7S-</chem>	294.06530		9.26	Monoterpene NOSSs and Sesquiterpene NOSSs

203 This quantification approach introduces inherent uncertainty, as differences in molecular  
 204 structure and functional groups between a surrogate and detected OSs have different ionization  
 205 efficiency (Ma et al., 2025), which is a well-documented challenge in NTA of complex mixtures.  
 206 However, this approach provides a consistent basis for comparing the relative abundance of OS in  
 207 different cities and their formation driving factors. Hence, the mass concentration of detected OSs is  
 208 still reliable in understanding their classification and formation driving factors.

209 To classify the Unknown OSs, we first calculated the  $X_c$  of each species. Those with  $DBE > 2$  and  
 210  $X_c > 2.50$  were designated as Aromatic OSs (Yassine et al., 2014). Subsequently, constrained positive  
 211 matrix factorization (PMF) analysis was performed using EPA PMF 5.0. The input matrix comprised  
 212 the mass concentrations of 60 unclassified OS species across all samples.

213 Figure S2 shows the source profiles of PMF model. Four factors were identified in this study.  
 214 Specifically, Factor 1 is identified as Aliphatic OSs due to the dominant contributions from species  
 215 like C11H22O5S and C12H24O5S, which possess low DBE and are characteristic of long-chain alkane  
 216 oxidation (Yang et al., 2024). This assignment is strongly supported by the co-variation of this factor  
 217 with n-dodecane. Similarly, Factor 2 is classified as Aromatic OSs, highlighted by the significant  
 218 contribution of C10H10O7S and C11H14O7S, which have been proved as OSs derived from typical  
 219 aromatic VOCs (Riva et al., 2015). In addition, the high contributions of benzene, toluene, and styrene  
 220 in Factor 2 further suggests that this factor should be classified as Aromatic OSs. As for Factor 3 and  
 221 Factor 4 is confirmed by the prominence of established Monoterpene OSs (Surratt et al., 2008; Iinuma  
 222 et al., 2007) (e.g., C10H18O5S, C10H17NO7S) and Sesquiterpene OSs (Wang et al., 2022b) (e.g.,  
 223 C14H28O6S, C15H25NO7S), respectively. Moreover, isoprene showed high contribution in both Factors  
 224 3 and 4. As monoterpenes and sesquiterpenes cannot be detected by online GC-MS, considering that  
 225 monoterpenes and sesquiterpenes mainly originate from biogenic sources and strongly correlate with  
 226 isoprene (Guenther et al., 2006; Sakulyanontvittaya et al., 2008), therefore, isoprene is used as a  
 227 surrogate marker as Monoterpene OSs and Sesquiterpene OSs. High contribution of isoprene in  
 228 Factors 3 and 4 proved that these factors were respectively determined as Monoterpene OSs and  
 229 Sesquiterpene OSs. Based on marker species, Unknown OSs were further categorized into  
 230 Monoterpene, Aromatic, Aliphatic, and Sesquiterpene OSs.

231 The model was executed with 10 runs to ensure stability. The ratio of  $Q_{robust}/Q_{true}$  for this solution  
 232 was stabilized below 1.50, indicating a robust fit without over-factorization. Furthermore, the scaled

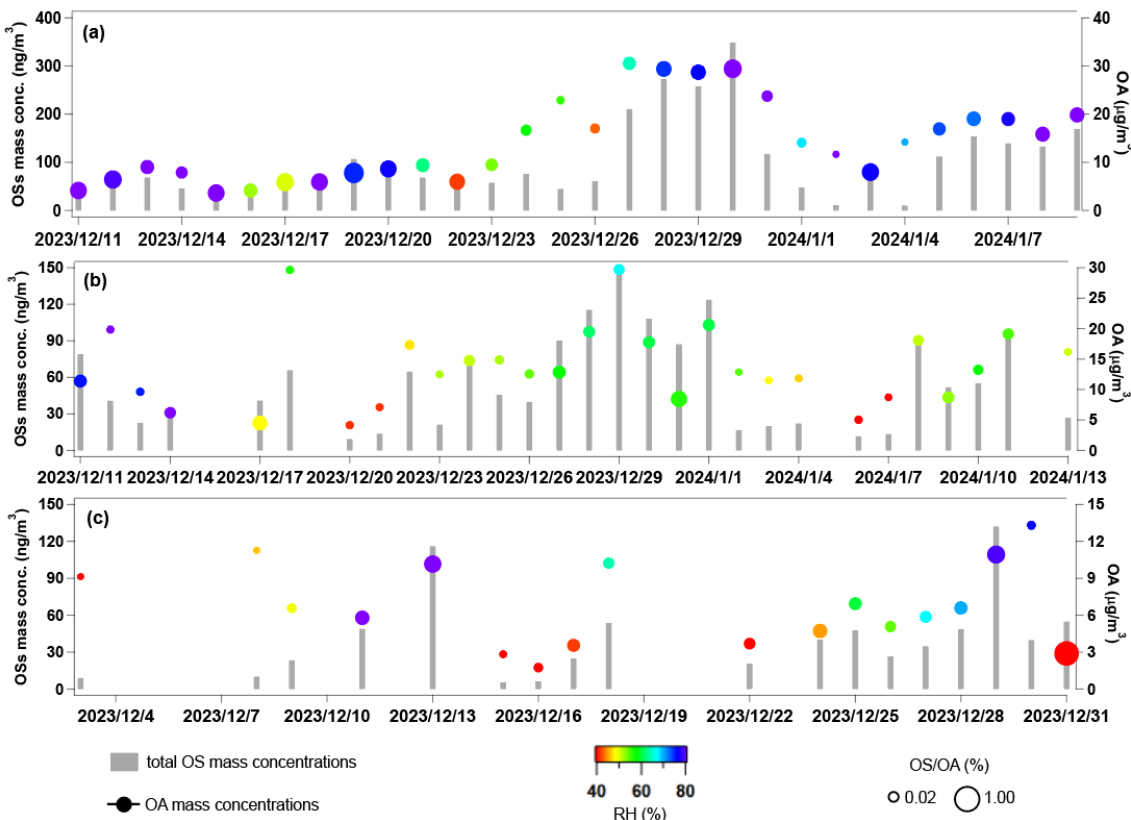
residual matrix (see Figure S3), demonstrating that residuals are randomly distributed and predominantly within the acceptable range of -3 to 3. Correlation coefficients between classified OSs and corresponding VOCs (Monoterpene OSs vs. isoprene; Aromatic OSs vs. benzene; Aliphatic OSs vs. n-dodecane; Sesquiterpene OSs vs. isoprene) were calculated as a statistical auxiliary variable to verify the reliability of PMF results. The arithmetic mean of hourly VOCs within each corresponding filter sampling period was calculated to align the time resolution of VOCs and OS mass concentration. Species with  $R < 0.40$  were excluded to avoid potential incorrect classification.

To validate classification accuracy,  $MS^2$  fragment patterns were analyzed (Table S5). Diagnostic fragments supported the assignments: Aliphatic OSs showed sequential alkyl chain cleavages ( $\Delta m/z = 14.0157$ ) and saturated alkyl fragments ( $[C_nH_{2n+1}]^-$  or  $[C_nH_{2n-1}]^+$ ); Monoterpene OSs displayed  $[C_nH_{2n-3}]^+$  fragments; Aromatic OSs exhibited characteristic aromatic substituent fragments ( $[C_6H_5R-H]^-$ , R = alkyl, carbonyl, -OH, or H). While absolute certainty for every individual OS in a complex ambient mixture is unattainable, integrating the precursor-constrained PMF model, tracer VOCs correlation analysis, and  $MS^2$  fragment patterns validation significantly reduces the likelihood of systematic misclassification.

### 3. Results and Discussion

#### 3.1 Concentrations, Compositions, and Classification of Organosulfates

Figure 1 shows the temporal variations of OS and organic aerosols (OA) mass concentrations, as well as RH, during the sampling period across the three cities. The total mass concentration of OS reported in this study is the sum of the (semi-)quantified concentrations of all individual OS species that met the identification criteria described in Section 2.3. The mean OSs concentrations were  $(41.1 \pm 34.5) \text{ ng/m}^3$  in Beijing,  $(57.4 \pm 39.2) \text{ ng/m}^3$  in Taiyuan, and  $(102.1 \pm 80.5) \text{ ng/m}^3$  in Changsha. Table S6 summarizes the average concentrations of  $PM_{2.5}$ , OC, gaseous pollutants, OS mass concentrations, and the mean meteorological parameters during sampling period for all three cities. OS accounted for  $0.64\% \pm 0.44\%$ ,  $0.41\% \pm 0.24\%$ , and  $0.76\% \pm 0.34\%$  of the total OA in Beijing, Taiyuan, and Changsha, respectively.



259  
260 **Figure 1** Temporal variations of daily total OS mass concentrations and average OA mass  
261 concentrations in (a) Changsha, (b) Taiyuan, and (c) Beijing. The markers of OA mass concentrations  
262 are colored by average RH during sampling period, and marker sizes indicate the OS/OA mass  
263 concentration ratios.

264 The highest OS mass concentrations and OS/OA ratios were observed in Changsha. As shown in  
265 Figure 1(a), a distinct episode with OS mass concentrations exceeding  $300 \text{ ng/m}^3$  occurred between  
266 December 27<sup>th</sup> and 31<sup>st</sup>, leading to the elevated OS mass concentrations in Changsha. This episode  
267 coincided with a period of intense fireworks activity, as evidenced by significant increases in the  
268 concentrations of recognized fireworks tracers, especially Ba and K (see Figure S4), leading to an  
269 increase in  $\text{SO}_2$  emission. We noted that though K may originate from biomass burning, its trend in  
270 concentration shows good consistency with that of Ba. Therefore, we still infer that fireworks activity  
271 are also the primary source of K. Considering persistently high RH (consistently  $>70\%$ ) during this  
272 period, as displayed in Figure S5, ALWC ( $117.9 \mu\text{g/m}^3$  in average) therefore increased and facilitated  
273 the heterogeneous oxidation of  $\text{SO}_2$  to particulate sulfate (Wang et al., 2016a; Ye et al., 2023). Since  
274 particulate sulfate serves as a key reactant in OS formation pathways, its elevated concentration  
275 directly promoted OS production (Xu et al., 2024; Wang et al., 2020). Furthermore, fireworks activity  
276 led to concurrent increases in the concentrations of transition metals, notably Fe and Mn (Figure S4),  
277 which are known to catalyze aqueous-phase radical chemistry and OS formation (Huang et al., 2019;  
278 Huang et al., 2018a). Therefore, the pronounced OS mass concentration during this period is attributed  
279 to a combination of elevated precursor emissions ( $\text{SO}_2$ ), high-RH conditions favoring aqueous-phase  
280 processing, and the potential catalytic role of co-emitted transition metals.

281 It is noteworthy that the single highest OS/OA ratio in Beijing was observed on December 31<sup>st</sup>  
282 under low RH. This phenomena highlights that ALWC, while a major driving factor of OS formation,

283 is not an exclusive control. Specifically, this day showed high atmospheric oxidative capacity and  
284 aerosol acidity. We note that under such conditions, efficient acid-catalyzed heterogeneous reactions  
285 of gas-phase oxidation products could drive substantial OS formation. The impact of ALWC,  
286 atmospheric oxidative capacity, and aerosol pH on OS formation will be discussed in detail in Section  
287 3.2.

288 Figures 2(a) and 2(b) shows the average mass concentrations and fractions of different OSs  
289 categories across the three cities, based on classification approach based on OSs' elemental  
290 composition and laboratory chamber-derived precursor–OS relationships and our precursor-based  
291 PMF classification approach developed in this work, respectively (see Section 2.3 for details). As  
292 displayed in Figure 2(b), Monoterpene OSs dominated detected OSs across all cities, contributing 55.2%  
293 (Beijing), 46.8% (Taiyuan), and 72.3% (Changsha) to total OS, respectively. Biogenic-emitted  
294 monoterpene is the precursor of Monoterpene OSs. However, monoterpene are primarily biogenic  
295 precursors, their limited emissions during winter cannot fully explain the high mass fractions of  
296 Monoterpene OSs. Recent studies have highlighted anthropogenic sources, particularly biomass  
297 burning, as significant contributors to monoterpene (Wang et al., 2022a; Koss et al., 2018). The PM<sub>2.5</sub>  
298 source apportionment analysis (Text S2, Figure S6) confirmed that biomass burning substantially  
299 contributed to PM<sub>2.5</sub> across all cities. The highest total mass fractions of Monoterpene OSs in  
300 Changsha are mainly attributed to the high RH (Table S6), which facilitates their formation via  
301 heterogeneous reactions (Hettiyadura et al., 2017; Wang et al., 2018; Ding et al., 2016a; Ding et al.,  
302 2016b; Li et al., 2020).

303 In Taiyuan, the total mass fractions of Aromatic OSs (21.2%) were significantly higher than those  
304 in Beijing (10.7%) and Changsha (4.6%). Aromatic OSs primarily formed via aqueous-phase reactions  
305 between S(IV) and aromatic VOCs (Huang et al., 2020). Taiyuan exhibited the highest sulfate mass  
306 concentration among the three cities (Table S6), which promoted the formation of these species.  
307 Additionally, transition metal ions—particularly Fe<sup>3+</sup>—catalyze aqueous-phase formation of Aromatic  
308 OSs (Huang et al., 2020). High Fe mass concentration was observed in Taiyuan (0.79 ± 0.53 µg/m<sup>3</sup>),  
309 further facilitated the formation of Aromatic OSs.

310 The highest total mass fractions of Aliphatic OSs were observed in Beijing (28.1%). Since vehicle  
311 emissions, which is an important source of long-chain alkenes (He et al., 2022; Wang et al., 2021a;  
312 Riva et al., 2016b; Tao et al., 2014; Tang et al., 2020), substantially contributed to PM<sub>2.5</sub> in all cities  
313 (Figure S6), the relative dominance of Aliphatic OSs in Beijing can be attributed to a comparative  
314 reduction in the emissions of precursors for Monoterpene OSs and Aromatic OSs. Specifically, Beijing  
315 exhibits lower emissions of monoterpene and aromatic VOCs precursors relative to Taiyuan and  
316 Changsha, which results in a reduced contribution of Monoterpene and Aromatic OSs to the total OS  
317 (see Figure 2(b)). Therefore, the relative mass fraction of Aliphatic OSs, which primarily derived from  
318 between sulfate and photooxidation products of alkenes (Riva et al., 2016b), becomes more prominent  
319 in Beijing. Additionally, low RH in Beijing further suppresses the aqueous-phase formation of  
320 Monoterpene OSs, amplifying the relative importance of Aliphatic OSs.

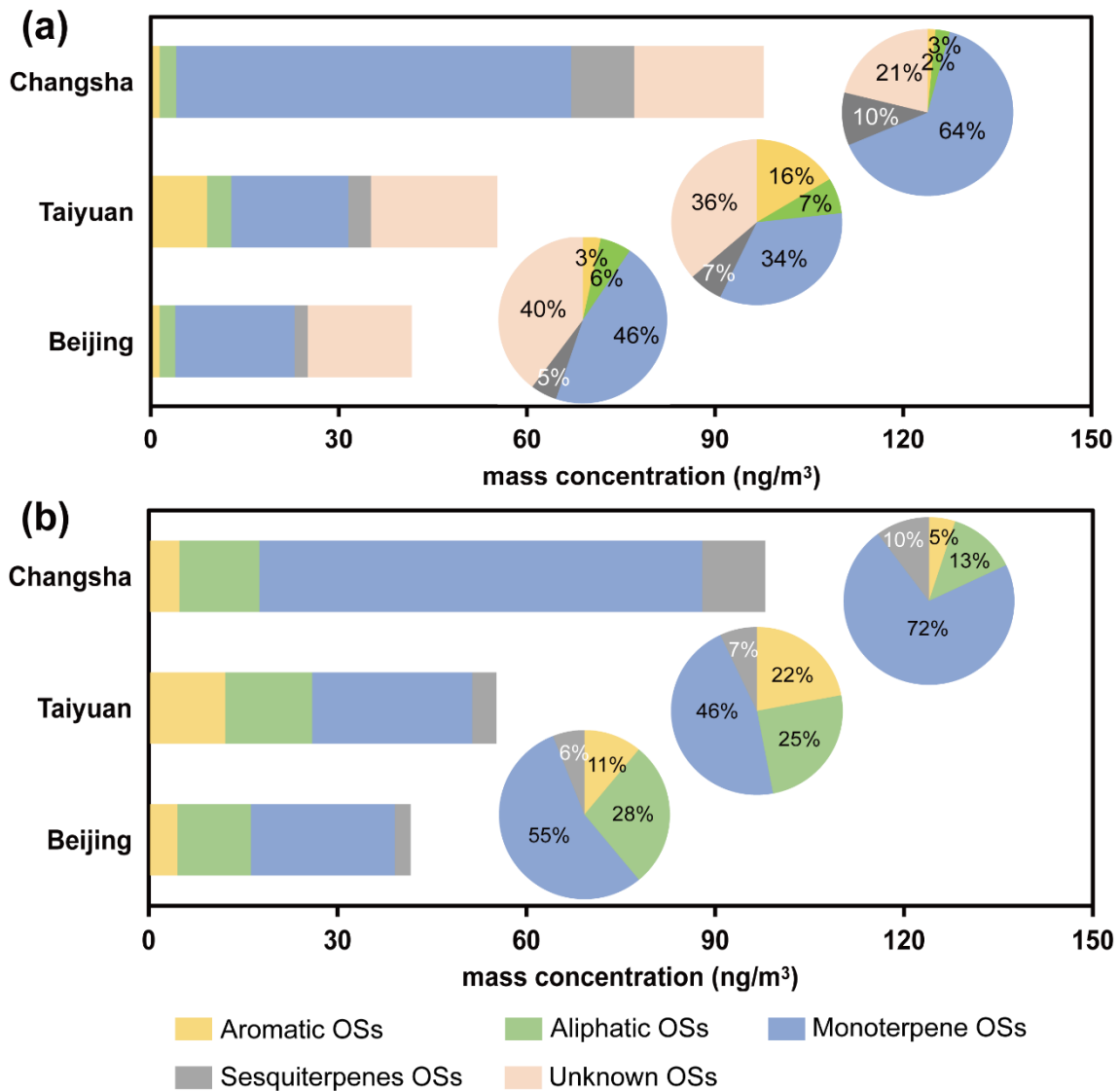


**Figure 2** The average mass concentrations of different OSs categories using (a) conventional classification approach based on OSs' elemental composition and laboratory chamber-derived precursor–OS relationships and (b) precursor-based PMF classification approach developed in this work across all cities. The inserted pie chart indicates the average mass fractions of different OSs categories.

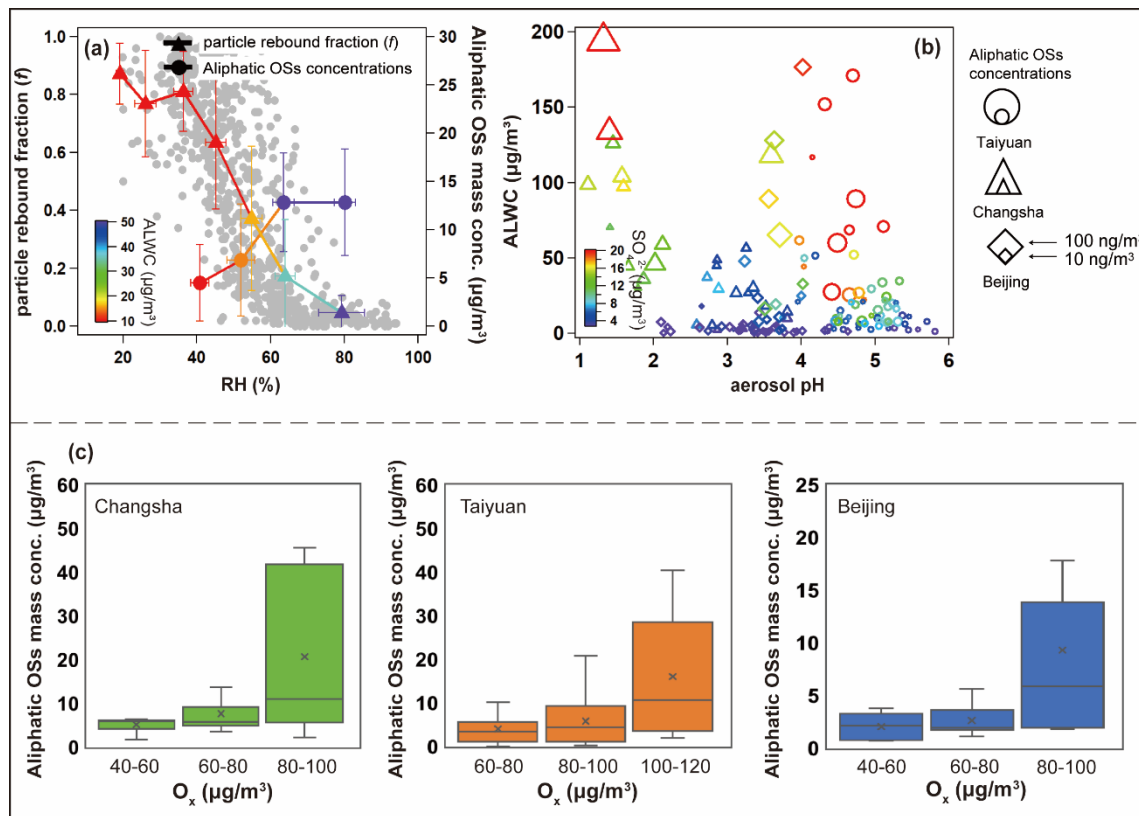
### 3.2 Formation Driving Factors of Aliphatic OSs and NOSSs

Compared with conventional classification approach (Figure 2(a)), we found Aliphatic OSs increased markedly (by 22.0%, 17.8%, and 10.3% in Beijing, Taiyuan, and Changsha, respectively). Therefore, we further examined the formation drivers of Aliphatic OSs.

ALWC plays a key role in facilitate OSs formation (Wang et al., 2020). Using  $PM_{2.5}$  chemical composition and RH, ALWC was calculated via the ISORROPIA-II model (details in Text S3) (Fountoukis and Nenes, 2007). Given the direct influence of ambient RH on ALWC (Figure S7) (Bateman et al., 2014) and leveraging RH-resolved samples from Beijing and Taiyuan, we assessed RH effects on Aliphatic OSs under low ( $RH < 40\%$ ), medium ( $40\% \leq RH < 60\%$ ), and high ( $RH \geq 60\%$ ).

336 60%) conditions.

337 In Changsha, where RH remains consistently high, Aliphatic OSs mass concentrations strongly  
338 correlated with RH ( $R = 0.78$ ). In Beijing and Taiyuan, correlations increased from low to medium  
339 RH (Beijing: 0.53 to 0.82; Taiyuan: 0.38 to 0.77) but declined slightly at higher RH (Beijing: 0.82 to  
340 0.69; Taiyuan: 0.77 to 0.72). The initial correlation rise reflects ALWC-enhanced sulfate-driven  
341 heterogeneous OS formation (Wang et al., 2016b; Cheng et al., 2016b), while the decline at elevated  
342 RH may due to the increase in ALWC dilutes the concentrations of precursors and intermediates of  
343 Aliphatic OSs within the aqueous phase. Therefore, Aliphatic OSs formation were not further  
344 promoted, exhibiting the non-linear response of their mass concentrations and ALWC.



345

346 **Figure 3** (a) The measured particle rebound fraction ( $f$ ) and total mass concentrations of Aliphatic OSs  
347 as a function of RH, the plots were colored by the calculated ALWC concentrations in Taiyuan, grey  
348 dots indicate the mass concentrations of Aliphatic OSs; (b) the relationship between aerosol pH and  
349 ALWC across three cities, the markers were colored by the inorganic sulfate mass concentrations, the  
350 marker sizes represented the total mass concentrations of Aliphatic OSs; (c) the box plot of total mass  
351 concentrations of Aliphatic OSs at different  $\text{O}_x$  concentration levels.

352 This threshold behavior aligns with aerosol phase transitions. Particle rebound fraction ( $f$ ),  
353 indicating phase state, was measured in Taiyuan using a three-arm impactor (Liu et al., 2017). As RH  
354 exceeded 60%,  $f$  dropped below 0.2 (Figure 3(a)), signaling a transition from non-liquid to liquid  
355 aerosol states. This transition at  $\text{RH} > 60\%$  aligns with prior field (Liu et al., 2017; Liu et al., 2023;  
356 Meng et al., 2024; Song et al., 2022) and modeling (Qiu et al., 2023) studies in Eastern China.  
357 Correspondingly, Aliphatic OSs concentrations increased with RH below 60% but plateaued beyond  
358 that despite further humidity rises. These findings underscore aerosol phase state as a critical factor:

359 initial liquid phase formation (RH < 60%) promotes heterogeneous OS formation (Ye et al., 2018),  
360 whereas at higher RH, saturation of reactive interfaces limits further ALWC effects.

361 In addition, the increase in ALWC with rising RH altered aerosol pH (Figure 3(b)), which  
362 inhibited OSs formation via acid-catalyzed reactions (Duporté et al., 2016). In Changsha, as aerosol  
363 pH increased from approximately 1.0 to above 3.0, the average total mass concentrations of Aliphatic  
364 OSs decreased significantly from 9.3 to 4.6 ng/m<sup>3</sup> (Figure S8), with further declines as pH increased.  
365 In Taiyuan, OS concentrations dropped from 12.2 to 6.8 ng/m<sup>3</sup> as pH rose from below 4.5 to above  
366 5.0. However, in Beijing, total mass concentrations of Aliphatic OSs remained stable within a narrow  
367 pH range of 3.2–3.9. Elevated ALWC facilitates aqueous-phase radical chemistry that forms OSs via  
368 non-acid pathways, which can dominate over pH-dependent processes (Rudziński et al., 2009; Wach  
369 et al., 2019; Huang et al., 2019). Thus, pH-dependent suppression of Aliphatic OSs formation is  
370 common across urban aerosol pH ranges, but less evident when pH varies narrowly.

371 Inorganic sulfate plays a crucial role in OSs formation via sulfate esterification reactions (Xu et  
372 al., 2024; Wang et al., 2020). We thus examined its effect on the formation of Aliphatic OSs. Figure  
373 3(b) illustrates the relationships among ALWC, pH, inorganic sulfate mass concentration, and total  
374 mass concentrations of Aliphatic OSs across all cities. A consistent positive correlation was observed,  
375 consistent with previous field studies (Lin et al., 2022; Wang et al., 2023b; Le Breton et al., 2018;  
376 Wang et al., 2018). This correlation was strongest when sulfate concentrations were below 20 µg/m<sup>3</sup>.  
377 Below this threshold, total mass concentrations of Aliphatic OSs increased significantly with inorganic  
378 sulfate, whereas above it, the correlation weakened. Additionally, inorganic sulfate mass concentration  
379 showed a clear positive correlation with ALWC (Figure 3(b)), suggesting that ionic strength did not  
380 increase linearly with sulfate mass. This likely reflects saturation effects in acid-mediated pathways,  
381 driven by limitations in water activity and ionic strength (Wang et al., 2020). Overall, these results  
382 highlight the nonlinear influence of inorganic sulfate on Aliphatic OSs formation.

383 Atmospheric oxidative capacity, represented by O<sub>x</sub> (O<sub>x</sub> = O<sub>3</sub> + NO<sub>2</sub>) concentrations, typically  
384 modulates OS formation via acid-catalyzed ring-opening reactions pathways. As shown in Figure 3(c),  
385 total mass concentrations of Aliphatic OSs and NOSs exhibited significant increases with rising O<sub>x</sub>  
386 levels across all cities. Especially, total mass concentrations of Aliphatic OSs significantly increased  
387 across all cities when O<sub>x</sub> concentrations raised from 60–80 µg/m<sup>3</sup> to > 80 µg/m<sup>3</sup>. As shown in Figure  
388 S9, O<sub>3</sub> dominated the O<sub>x</sub> composition during high-O<sub>x</sub> episodes (> 80 µg/m<sup>3</sup>) across all cities. Previous  
389 laboratory studies have suggested that enhanced atmospheric oxidation capacities promote the  
390 oxidation of VOCs (Zhang et al., 2022; Wei et al., 2024), forming cyclic intermediates. We therefore  
391 inferred that the increase in O<sub>x</sub> facilitates the formation of cyclic intermediates derived from long-  
392 chain alkenes. Subsequent acid-catalyzed and ring-opening reactions are important pathways of  
393 heterogeneous OSs formation, including Aliphatic OSs (Eddingsaas et al., 2010; Iinuma et al., 2007;  
394 Brüggemann et al., 2020).

395 It should be noted that though formation driving factors of Aliphatic OSs identified in this work,  
396 including ALWC, inorganic sulfate, and O<sub>x</sub>, are likely applicable in other urban environments sharing  
397 similar winter conditions characterized by high anthropogenic emissions and moderate-to-high  
398 humidity. However, their importance may differ in other cities with different atmospheric conditions,  
399 like in summer with strong biogenic emissions, in regions with low aerosol acidity, or in arid cities  
400 with persistently low RH.

---

401    **4 Conclusions and Implications**

402    In this study, we applied a NTA approach based on UHPLC-HRMS to investigate the molecular  
403    composition of OS in PM<sub>2.5</sub> samples from three cities. By integrating molecular composition data,  
404    precursor-constrained PMF source apportionment, and OS-precursor correlation analysis, we  
405    developed a comprehensive method for accurate classification of detected OSs, demonstrating  
406    superior discrimination between Aliphatic OSs. Conventional classification methods rely on  
407    laboratory chamber-derived precursor-OS relationships (Wang et al., 2019a), which provide limited  
408    insight into the formation of Aliphatic OSs and tend to underestimate their mass fractions. The  
409    abundant Aliphatic OSs detected in ambient PM<sub>2.5</sub> suggest complex formation pathways, such as OH  
410    oxidation of long-chain alkenes (Riva et al., 2016b) and heterogeneous reactions between SO<sub>2</sub> and  
411    alkene reactions in acidic environments conditions (Passananti et al., 2016), which remain  
412    incompletely understood in laboratory studies. Our findings highlight the importance of emphasizing  
413    the formation of Aliphatic OSs in urban atmospheres.

414

415    ~~However, this study still faces several challenges. This work was conducted during the winter.~~  
416    OS formation exhibits seasonal variability, particularly for pathways driven by biogenic VOCs  
417    emissions and photochemical activity, which are generally enhanced in warmer months. Hence, the  
418    underestimation of Aliphatic OSs, and their key formation factors determined in this work remain  
419    valid insights for the winter period but may not fully represent annual OS behavior. Hence  
420    In addition, our field campaigns were conducted in three typical different Chinese cities, the effect of these driving  
421    factors on the formation of Aliphatic OSs may not be applicable to other cities with different  
422    atmospheric conditions.~~the underestimation of Aliphatic OSs, and their key formation factors~~  
423    ~~determined in this work remain valid insights for the winter period but may not fully represent annual~~  
424    ~~OS behavior.~~ Future long-term observations in more cities are necessary to resolve the complete  
425    annual cycle of OS composition, quantify the shifting contributions of anthropogenic versus biogenic  
426    precursors, and understanding how key formation driving factors evolve with changing atmospheric  
427    conditions.

428    For NTA, the use of surrogate standards for quantification OS mass concentration introduced  
429    uncertainty, particularly due to the extraction efficiency of individual OSs species from quartz fiber  
430    filters could not be determined. Although we have adopted standardized extraction protocol ensures  
431    high comparability across our samples, absolute extraction recoveries may vary. In addition, this  
432    approach depends on public molecular composition such as mzCloud and ChemSpider integrated  
433    within the Compound Discoverer software, which contain limited entries for organosulfates. Reliance  
434    on these databases for compound identification may therefore underestimate OS mass concentrations  
435    in urban environments. For example, OSs identified here accounted for less than 1% of total OA mass,  
436    whereas recent work (Ma et al., 2025) reported approximately 20% contributions.

437    OS may become increasingly significant in OA, particularly in coastal regions influenced by  
438    oceanic dimethyl sulfate emissions (Brüggemann et al., 2020). Our future work will focus on  
439    synthesizing OSs standards representing various precursors and establishing a dedicated fragmentation  
440    database through multi-platform MS<sup>2</sup> validation to elucidate OS sources in more detail.

---

441 **Author Contributions**

442 Y.Q., J.W., and Z.W. designed this work. J.L., Y.Wei, C.L., J.Y., T.L., R.M., T.Z., W.F., J.Y., Z.F., Y.X.  
443 and K.B. collected PM<sub>2.5</sub> samples. Y.Q., J.W., T.Q., Y.B., and D.L. conducted UHPLC-HRMS  
444 experiments. Y.Q., J.W., Z.G., and Y.Wang wrote this manuscript. Z.W., Y.Wang, and M.H. edited this  
445 manuscript. All authors have read and agreed to submit this manuscript. Y.Q. and J.W. contributed  
446 equally to this work.

447 **Funding**

448 This work is funded by the National Nature Science Foundation of China (Grants 22221004 and  
449 22306059), This work was also supported by the Science and Technology Innovation Program of  
450 Hunan Province (Grants 2024RC3106 and 2025AQ2001), and the Fundamental Research Funds  
451 for the Central Universities (Grant 531118010830).

452 **Notes**

453 The authors declare that they have no conflict of interest.

454 **Acknowledgements**

455 Y.W would like to acknowledge financial support by the National Nature Science Foundation of  
456 China (Grants 22221004 and 22306059), This work was also supported by the Science and  
457 Technology Innovation Program of Hunan Province (Grants 2024RC3106 and 2025AQ2001),  
458 and the Fundamental Research Funds for the Central Universities (Grant 531118010830).

459

---

460      **References**

461      Bateman, A. P., Belassein, H., Martin, S. T.: Impactor Apparatus for the Study of Particle Rebound:  
462      Relative Humidity and Capillary Forces. *Aerosol Science and Technology*. 48, 42-52.  
463      10.1080/02786826.2013.853866, 2014.

464      Brown, S. S., Dubé, W. P., Karamchandani, P., Yarwood, G., Peischl, J., Ryerson, T. B., Neuman, J. A.,  
465      Nowak, J. B., Holloway, J. S., Washenfelder, R. A., Brock, C. A., Frost, G. J., Trainer, M., Parrish, D. D.,  
466      Fehsenfeld, F. C., Ravishankara, A. R.: Effects of NO<sub>x</sub> control and plume mixing on nighttime chemical  
467      processing of plumes from coal-fired power plants. *Journal of Geophysical Research: Atmospheres*. 117.  
468      <https://doi.org/10.1029/2011JD016954>, 2012.

469      Brüggemann, M., Xu, R., Tilgner, A., Kwong, K. C., Mutzel, A., Poon, H. Y., Otto, T., Schaefer, T.,  
470      Poulain, L., Chan, M. N., Herrmann, H.: Organosulfates in Ambient Aerosol: State of Knowledge and  
471      Future Research Directions on Formation, Abundance, Fate, and Importance. *Environmental Science &*  
472      *Technology*. 54, 3767-3782. 10.1021/acs.est.9b06751, 2020.

473      Cai, D., Wang, X., Chen, J., Li, X.: Molecular Characterization of Organosulfates in Highly Polluted  
474      Atmosphere Using Ultra-High-Resolution Mass Spectrometry. *Journal of Geophysical Research: Atmospheres*. 125, e2019JD032253. <https://doi.org/10.1029/2019JD032253>, 2020.

476      Cao, G., Zhao, X., Hu, D., Zhu, R., Ouyang, F.: Development and application of a quantification  
477      method for water soluble organosulfates in atmospheric aerosols. *Environmental Pollution*. 225, 316-322.  
478      <https://doi.org/10.1016/j.envpol.2017.01.086>, 2017.

479      Cheng, Y., Zheng, G., Wei, C., Mu, Q., Zheng, B., Wang, Z., Gao, M., Zhang, Q., He, K., Carmichael,  
480      G., Pöschl, U., Su, H.: Reactive nitrogen chemistry in aerosol water as a source of sulfate during haze events  
481      in China. *Science Advances*. 2, e1601530. 10.1126/sciadv.1601530, 2016a.

482      Cheng, Y., Zheng, G., Wei, C., Mu, Q., Zheng, B., Wang, Z., Gao, M., Zhang, Q., He, K., Carmichael,  
483      G., Pöschl, U., Su, H.: Reactive nitrogen chemistry in aerosol water as a source of sulfate during haze events  
484      in China. 2, e1601530. doi:10.1126/sciadv.1601530, 2016b.

485      Deng, Y., Inomata, S., Sato, K., Ramasamy, S., Morino, Y., Enami, S., Tanimoto, H.: Temperature and  
486      acidity dependence of secondary organic aerosol formation from  $\alpha$ -pinene ozonolysis with a compact  
487      chamber system. *Atmos. Chem. Phys.* 21, 5983-6003. 10.5194/acp-21-5983-2021, 2021.

488      Ding, X., He, Q.-F., Shen, R.-Q., Yu, Q.-Q., Zhang, Y.-Q., Xin, J.-Y., Wen, T.-X., Wang, X.-M.: Spatial  
489      and seasonal variations of isoprene secondary organic aerosol in China: Significant impact of biomass  
490      burning during winter. *Scientific Reports*. 6, 20411. 10.1038/srep20411, 2016a.

491      Ding, X., Zhang, Y.-Q., He, Q.-F., Yu, Q.-Q., Shen, R.-Q., Zhang, Y., Zhang, Z., Lyu, S.-J., Hu, Q.-H.,  
492      Wang, Y.-S., Li, L.-F., Song, W., Wang, X.-M.: Spatial and seasonal variations of secondary organic aerosol  
493      from terpenoids over China. *Journal of Geophysical Research: Atmospheres*. 121, 14,661-614,678.  
494      <https://doi.org/10.1002/2016JD025467>, 2016b.

495      Duporté, G., Flaud, P. M., Geneste, E., Augagneur, S., Pangui, E., Lamkaddam, H., Gratien, A.,  
496      Doussin, J. F., Budzinski, H., Villenave, E., Perraudin, E.: Experimental Study of the Formation of

497 Organosulfates from  $\alpha$ -Pinene Oxidation. Part I: Product Identification, Formation Mechanisms and Effect  
498 of Relative Humidity. *The Journal of Physical Chemistry A.* 120, 7909-7923. 10.1021/acs.jpca.6b08504,  
499 2016.

500 Duporté, G., Flaud, P. M., Kammer, J., Geneste, E., Augagneur, S., Pangui, E., Lamkaddam, H.,  
501 Gratien, A., Doussin, J. F., Budzinski, H., Villenave, E., Perrauidin, E.: Experimental Study of the Formation  
502 of Organosulfates from  $\alpha$ -Pinene Oxidation. 2. Time Evolution and Effect of Particle Acidity. *The Journal of  
503 Physical Chemistry A.* 124, 409-421. 10.1021/acs.jpca.9b07156, 2020.

504 Eddingsaas, N. C., VanderVelde, D. G., Wennberg, P. O.: Kinetics and Products of the Acid-Catalyzed  
505 Ring-Opening of Atmospherically Relevant Butyl Epoxy Alcohols. *The Journal of Physical Chemistry A.*  
506 114, 8106-8113. 10.1021/jp103907c, 2010.

507 Edwards, P. M., Aikin, K. C., Dube, W. P., Fry, J. L., Gilman, J. B., de Gouw, J. A., Graus, M. G.,  
508 Hanisco, T. F., Holloway, J., Hübner, G., Kaiser, J., Keutsch, F. N., Lerner, B. M., Neuman, J. A., Parrish,  
509 D. D., Peischl, J., Pollack, I. B., Ravishankara, A. R., Roberts, J. M., Ryerson, T. B., Trainer, M., Veres, P.  
510 R., Wolfe, G. M., Warneke, C., Brown, S. S.: Transition from high- to low-NO<sub>x</sub> control of night-time  
511 oxidation in the southeastern US. *Nature Geoscience.* 10, 490-495. 10.1038/ngeo2976, 2017.

512 Estillore, A. D., Hettiyadura, A. P. S., Qin, Z., Leckrone, E., Wombacher, B., Humphry, T., Stone, E.  
513 A., Grassian, V. H.: Water Uptake and Hygroscopic Growth of Organosulfate Aerosol. *Environmental  
514 Science & Technology.* 50, 4259-4268. 10.1021/acs.est.5b05014, 2016.

515 Fleming, L. T., Ali, N. N., Blair, S. L., Roveretto, M., George, C., Nizkorodov, S. A.: Formation of  
516 Light-Absorbing Organosulfates during Evaporation of Secondary Organic Material Extracts in the  
517 Presence of Sulfuric Acid. *ACS Earth and Space Chemistry.* 3, 947-957.  
518 10.1021/acsearthspacechem.9b00036, 2019.

519 Fountoukis, C., Nenes, A.: ISORROPIA II: a computationally efficient thermodynamic equilibrium  
520 model for K<sup>+</sup>; Ca<sup>2+</sup>; Mg<sup>2+</sup>; NH<sup>4+</sup>; Na<sup>+</sup>; SO<sub>4</sub><sup>2-</sup>; NO<sub>3</sub><sup>-</sup>; Cl<sup>-</sup>; H<sub>2</sub>O aerosols. *Atmospheric Chemistry and  
521 Physics.* 7, 4639-4659. 10.5194/acp-7-4639-2007, 2007.

522 Guenther, A., Karl, T., Harley, P., Wiedinmyer, C., Palmer, P. I., Geron, C.: Estimates of global  
523 terrestrial isoprene emissions using MEGAN (Model of Emissions of Gases and Aerosols from Nature).  
524 *Atmos. Chem. Phys.* 6, 3181-3210. 10.5194/acp-6-3181-2006, 2006.

525 Hansen, A. M. K., Hong, J., Raatikainen, T., Kristensen, K., Ylisirniö, A., Virtanen, A., Petäjä, T.,  
526 Glasius, M., Prisle, N. L.: Hygroscopic properties and cloud condensation nuclei activation of limonene-  
527 derived organosulfates and their mixtures with ammonium sulfate. *Atmos. Chem. Phys.* 15, 14071-14089.  
528 10.5194/acp-15-14071-2015, 2015.

529 He, J., Li, L., Li, Y., Huang, M., Zhu, Y., Deng, S.: Synthesis, MS/MS characteristics and quantification  
530 of six aromatic organosulfates in atmospheric PM<sub>2.5</sub>. *Atmospheric Environment.* 290, 119361.  
531 <https://doi.org/10.1016/j.atmosenv.2022.119361>, 2022.

532 Hettiyadura, A. P. S., Jayarathne, T., Baumann, K., Goldstein, A. H., de Gouw, J. A., Koss, A., Keutsch,  
533 F. N., Skog, K., Stone, E. A.: Qualitative and quantitative analysis of atmospheric organosulfates in  
534 Centreville, Alabama. *Atmospheric Chemistry and Physics.* 17, 1343-1359. 10.5194/acp-17-1343-2017,  
535 2017.

536 Hoyle, C. R., Boy, M., Donahue, N. M., Fry, J. L., Glasius, M., Guenther, A., Hallar, A. G., Huff Hartz,  
537 K., Petters, M. D., Petäjä, T., Rosenoern, T., Sullivan, A. P.: A review of the anthropogenic influence on  
538 biogenic secondary organic aerosol. *Atmos. Chem. Phys.* 11, 321-343. 10.5194/acp-11-321-2011, 2011.

539 Huang, L., Cochran, R. E., Coddens, E. M., Grassian, V. H.: Formation of Organosulfur Compounds  
540 through Transition Metal Ion-Catalyzed Aqueous Phase Reactions. *Environmental Science & Technology*  
541 Letters. 5, 315-321. 10.1021/acs.estlett.8b00225, 2018a.

542 Huang, L., Coddens, E. M., Grassian, V. H.: Formation of Organosulfur Compounds from Aqueous  
543 Phase Reactions of S(IV) with Methacrolein and Methyl Vinyl Ketone in the Presence of Transition Metal  
544 Ions. *ACS Earth and Space Chemistry*. 3, 1749-1755. 10.1021/acsearthspacechem.9b00173, 2019.

545 Huang, L., Liu, T., Grassian, V. H.: Radical-Initiated Formation of Aromatic Organosulfates and  
546 Sulfonates in the Aqueous Phase. *Environmental Science & Technology*. 54, 11857-11864.  
547 10.1021/acs.est.0c05644, 2020.

548 Huang, L., Wang, Y., Zhao, Y., Hu, H., Yang, Y., Wang, Y., Yu, J.-Z., Chen, T., Cheng, Z., Li, C., Li,  
549 Z., Xiao, H.: Biogenic and Anthropogenic Contributions to Atmospheric Organosulfates in a Typical  
550 Megacity in Eastern China. *Journal of Geophysical Research: Atmospheres*. 128, e2023JD038848.  
551 <https://doi.org/10.1029/2023JD038848>, 2023a.

552 Huang, L., Wang, Y., Zhao, Y., Hu, H., Yang, Y., Wang, Y., Yu, J.-Z., Chen, T., Cheng, Z., Li, C., Li,  
553 Z., Xiao, H.: Biogenic and Anthropogenic Contributions to Atmospheric Organosulfates in a Typical  
554 Megacity in Eastern China. 128, e2023JD038848. <https://doi.org/10.1029/2023JD038848>, 2023b.

555 Huang, R. J., Cao, J., Chen, Y., Yang, L., Shen, J., You, Q., Wang, K., Lin, C., Xu, W., Gao, B., Li, Y.,  
556 Chen, Q., Hoffmann, T., O'Dowd, C. D., Bilde, M., Glasius, M.: Organosulfates in atmospheric aerosol:  
557 synthesis and quantitative analysis of PM2.5 from Xi'an, northwestern China. *Atmos. Meas. Tech.* 11, 3447-  
558 3456. 10.5194/amt-11-3447-2018, 2018b.

559 Iinuma, Y., Müller, C., Berndt, T., Böge, O., Claeys, M., Herrmann, H.: Evidence for the Existence of  
560 Organosulfates from  $\beta$ -Pinene Ozonolysis in Ambient Secondary Organic Aerosol. *Environmental Science*  
561 & Technology. 41, 6678-6683. 10.1021/es070938t, 2007.

562 Jiang, H., Cai, J., Feng, X., Chen, Y., Guo, H., Mo, Y., Tang, J., Chen, T., Li, J., Zhang, G.:  
563 Organosulfur Compounds: A Non-Negligible Component Affecting the Light Absorption of Brown Carbon  
564 During North China Haze Events. *Journal of Geophysical Research: Atmospheres*. 130, e2024JD042043.  
565 <https://doi.org/10.1029/2024JD042043>, 2025.

566 Koss, A. R., Sekimoto, K., Gilman, J. B., Selimovic, V., Coggon, M. M., Zarzana, K. J., Yuan, B.,  
567 Lerner, B. M., Brown, S. S., Jimenez, J. L., Krechmer, J., Roberts, J. M., Warneke, C., Yokelson, R. J., de  
568 Gouw, J.: Non-methane organic gas emissions from biomass burning: identification, quantification, and  
569 emission factors from PTR-ToF during the FIREX 2016 laboratory experiment. *Atmos. Chem. Phys.* 18,  
570 3299-3319. 10.5194/acp-18-3299-2018, 2018.

571 Le Breton, M., Wang, Y., Hallquist, Å. M., Pathak, R. K., Zheng, J., Yang, Y., Shang, D., Glasius, M.,  
572 Bannan, T. J., Liu, Q., Chan, C. K., Percival, C. J., Zhu, W., Lou, S., Topping, D., Wang, Y., Yu, J., Lu, K.,  
573 Guo, S., Hu, M., Hallquist, M.: Online gas- and particle-phase measurements of organosulfates,  
574 organosulfonates and nitrooxy organosulfates in Beijing utilizing a FIGAERO ToF-CIMS. *Atmos. Chem.*

---

575 Phys. 18, 10355-10371. 10.5194/acp-18-10355-2018, 2018.

576 Li, L., Yang, W., Xie, S., Wu, Y.: Estimations and uncertainty of biogenic volatile organic compound  
577 emission inventory in China for 2008–2018. Science of The Total Environment. 733, 139301.  
578 <https://doi.org/10.1016/j.scitotenv.2020.139301>, 2020.

579 Lin, P., Yu, J. Z., Engling, G., Kalberer, M.: Organosulfates in Humic-like Substance Fraction Isolated  
580 from Aerosols at Seven Locations in East Asia: A Study by Ultra-High-Resolution Mass Spectrometry.  
581 Environmental Science & Technology. 46, 13118-13127. 10.1021/es303570v, 2012.

582 Lin, Y., Han, Y., Li, G., Wang, Q., Zhang, X., Li, Z., Li, L., Prévôt, A. S. H., Cao, J.: Molecular  
583 Characteristics of Atmospheric Organosulfates During Summer and Winter Seasons in Two Cities of  
584 Southern and Northern China. Journal of Geophysical Research: Atmospheres. 127, e2022JD036672.  
585 <https://doi.org/10.1029/2022JD036672>, 2022.

586 Liu, P., Ding, X., Li, B. X., Zhang, Y. Q., Bryant, D. J., Wang, X. M.: Quality assurance and quality  
587 control of atmospheric organosulfates measured using hydrophilic interaction liquid chromatography  
588 (HILIC). Atmos. Meas. Tech. 17, 3067-3079. 10.5194/amt-17-3067-2024, 2024.

589 Liu, Y., Wu, Z., Wang, Y., Xiao, Y., Gu, F., Zheng, J., Tan, T., Shang, D., Wu, Y., Zeng, L., Hu, M.,  
590 Bateman, A. P., Martin, S. T.: Submicrometer Particles Are in the Liquid State during Heavy Haze Episodes  
591 in the Urban Atmosphere of Beijing, China. Environ. Sci. Technol. Lett. 4, 427-432.  
592 10.1021/acs.estlett.7b00352, 2017.

593 Liu, Y. C., Wu, Z. J., Qiu, Y. T., Tian, P., Liu, Q., Chen, Y., Song, M., Hu, M.: Enhanced Nitrate Fraction:  
594 Enabling Urban Aerosol Particles to Remain in a Liquid State at Reduced Relative Humidity. Geophysical  
595 Research Letters. 50, e2023GL105505. <https://doi.org/10.1029/2023GL105505>, 2023.

596 Lukács, H., Gelencsér, A., Hoffer, A., Kiss, G., Horváth, K., Hartyáni, Z.: Quantitative assessment of  
597 organosulfates in size-segregated rural fine aerosol. Atmos. Chem. Phys. 9, 231-238. 10.5194/acp-9-231-  
598 2009, 2009.

599 Ma, J., Ungeheuer, F., Zheng, F., Du, W., Wang, Y., Cai, J., Zhou, Y., Yan, C., Liu, Y., Kulmala, M.,  
600 Daellenbach, K. R., Vogel, A. L.: Nontarget Screening Exhibits a Seasonal Cycle of PM2.5 Organic Aerosol  
601 Composition in Beijing. Environmental Science & Technology. 56, 7017-7028. 10.1021/acs.est.1c06905,  
602 2022.

603 Ma, J., Reininger, N., Zhao, C., Döbler, D., Rüdiger, J., Qiu, Y., Ungeheuer, F., Simon, M., D'Angelo,  
604 L., Breuninger, A., David, J., Bai, Y., Li, Y., Xue, Y., Li, L., Wang, Y., Hildmann, S., Hoffmann, T., Liu, B.,  
605 Niu, H., Wu, Z., Vogel, A. L.: Unveiling a large fraction of hidden organosulfates in ambient organic aerosol.  
606 Nature Communications. 16, 4098. 10.1038/s41467-025-59420-y, 2025.

607 Meng, X., Wu, Z., Chen, J., Qiu, Y., Zong, T., Song, M., Lee, J., Hu, M.: Particle phase state and  
608 aerosol liquid water greatly impact secondary aerosol formation: insights into phase transition and its role  
609 in haze events. Atmospheric Chemistry and Physics. 24, 2399-2414. 10.5194/acp-24-2399-2024, 2024.

610 Mutzel, A., Poulaïn, L., Berndt, T., Iinuma, Y., Rodigast, M., Böge, O., Richters, S., Spindler, G., Sipilä,  
611 M., Jokinen, T., Kulmala, M., Herrmann, H.: Highly Oxidized Multifunctional Organic Compounds  
612 Observed in Tropospheric Particles: A Field and Laboratory Study. Environmental Science & Technology.

613 49, 7754-7761. 10.1021/acs.est.5b00885, 2015.

614 Ohno, P. E., Wang, J., Mahrt, F., Varelas, J. G., Aruffo, E., Ye, J., Qin, Y., Kiland, K. J., Bertram, A.  
615 K., Thomson, R. J., Martin, S. T.: Gas-Particle Uptake and Hygroscopic Growth by Organosulfate Particles.  
616 ACS Earth and Space Chemistry. 6, 2481-2490. 10.1021/acsearthspacechem.2c00195, 2022.

617 Passananti, M., Kong, L., Shang, J., Dupart, Y., Perrier, S., Chen, J., Donaldson, D. J., George, C.:  
618 Organosulfate Formation through the Heterogeneous Reaction of Sulfur Dioxide with Unsaturated Fatty  
619 Acids and Long-Chain Alkenes. Angewandte Chemie International Edition. 55, 10336-10339.  
620 <https://doi.org/10.1002/anie.201605266>, 2016.

621 Qiu, Y., Liu, Y., Wu, Z., Wang, F., Meng, X., Zhang, Z., Man, R., Huang, D., Wang, H., Gao, Y., Huang,  
622 C., Hu, M.: Predicting Atmospheric Particle Phase State Using an Explainable Machine Learning Approach  
623 Based on Particle Rebound Measurements. Environmental Science & Technology. 57, 15055-15064.  
624 10.1021/acs.est.3c05284, 2023.

625 Riva, M., Tomaz, S., Cui, T., Lin, Y.-H., Perraудин, E., Gold, A., Stone, E. A., Villenave, E., Surratt, J.  
626 D.: Evidence for an Unrecognized Secondary Anthropogenic Source of Organosulfates and Sulfonates:  
627 Gas-Phase Oxidation of Polycyclic Aromatic Hydrocarbons in the Presence of Sulfate Aerosol.  
628 Environmental Science & Technology. 49, 6654-6664. 10.1021/acs.est.5b00836, 2015.

629 Riva, M., Budisulistiorini, S. H., Zhang, Z., Gold, A., Surratt, J. D.: Chemical characterization of  
630 secondary organic aerosol constituents from isoprene ozonolysis in the presence of acidic aerosol.  
631 Atmospheric Environment. 130, 5-13. <https://doi.org/10.1016/j.atmosenv.2015.06.027>, 2016a.

632 Riva, M., Da Silva Barbosa, T., Lin, Y. H., Stone, E. A., Gold, A., Surratt, J. D.: Chemical  
633 characterization of organosulfates in secondary organic aerosol derived from the photooxidation of alkanes.  
634 Atmospheric Chemistry and Physics. 16, 11001-11018. 10.5194/acp-16-11001-2016, 2016b.

635 Riva, M., Da Silva Barbosa, T., Lin, Y. H., Stone, E. A., Gold, A., Surratt, J. D.: Chemical  
636 characterization of organosulfates in secondary organic aerosol derived from the photooxidation of alkanes.  
637 Atmos. Chem. Phys. 16, 11001-11018. 10.5194/acp-16-11001-2016, 2016c.

638 Riva, M., Chen, Y., Zhang, Y., Lei, Z., Olson, N. E., Boyer, H. C., Narayan, S., Yee, L. D., Green, H.  
639 S., Cui, T., Zhang, Z., Baumann, K., Fort, M., Edgerton, E., Budisulistiorini, S. H., Rose, C. A., Ribeiro, I.  
640 O., e Oliveira, R. L., dos Santos, E. O., Machado, C. M. D., Szopa, S., Zhao, Y., Alves, E. G., de Sá, S. S.,  
641 Hu, W., Knipping, E. M., Shaw, S. L., Duvoisin Junior, S., de Souza, R. A. F., Palm, B. B., Jimenez, J.-L.,  
642 Glasius, M., Goldstein, A. H., Pye, H. O. T., Gold, A., Turpin, B. J., Vizuete, W., Martin, S. T., Thornton, J.  
643 A., Dutcher, C. S., Ault, A. P., Surratt, J. D.: Increasing Isoprene Epoxydiol-to-Inorganic Sulfate Aerosol  
644 Ratio Results in Extensive Conversion of Inorganic Sulfate to Organosulfur Forms: Implications for  
645 Aerosol Physicochemical Properties. Environmental Science & Technology. 53, 8682-8694.  
646 10.1021/acs.est.9b01019, 2019.

647 Rudziński, K. J., Gmachowski, L., Kuznietsova, I.: Reactions of isoprene and sulphony radical-anions  
648 – a possible source of atmospheric organosulphites and organosulphates. Atmos. Chem. Phys. 9, 2129-2140.  
649 10.5194/acp-9-2129-2009, 2009.

650 Sakulyanontvittaya, T., Guenther, A., Helmig, D., Milford, J., Wiedinmyer, C.: Secondary Organic  
651 Aerosol from Sesquiterpene and Monoterpene Emissions in the United States. Environmental Science &

---

652 Technology. 42, 8784-8790. 10.1021/es800817r, 2008.

653 Song, M., Jeong, R., Kim, D., Qiu, Y., Meng, X., Wu, Z., Zuend, A., Ha, Y., Kim, C., Kim, H., Gaikwad,  
654 S., Jang, K. S., Lee, J. Y., Ahn, J.: Comparison of Phase States of PM2.5 over Megacities, Seoul and Beijing,  
655 and Their Implications on Particle Size Distribution. Environmental Science and Technology. 56, 17581-  
656 17590. 10.1021/acs.est.2c06377, 2022.

657 Staudt, S., Kundu, S., Lehmler, H.-J., He, X., Cui, T., Lin, Y.-H., Kristensen, K., Glasius, M., Zhang,  
658 X., Weber, R. J., Surratt, J. D., Stone, E. A.: Aromatic organosulfates in atmospheric aerosols: Synthesis,  
659 characterization, and abundance. Atmospheric Environment. 94, 366-373.  
660 <https://doi.org/10.1016/j.atmosenv.2014.05.049>, 2014.

661 Surratt, J. D., Gómez-González, Y., Chan, A. W. H., Vermeylen, R., Shahgholi, M., Kleindienst, T. E.,  
662 Edney, E. O., Offenberg, J. H., Lewandowski, M., Jaoui, M., Maenhaut, W., Claeys, M., Flagan, R. C.,  
663 Seinfeld, J. H.: Organosulfate Formation in Biogenic Secondary Organic Aerosol. The Journal of Physical  
664 Chemistry A. 112, 8345-8378. 10.1021/jp802310p, 2008.

665 Tang, J., Li, J., Su, T., Han, Y., Mo, Y., Jiang, H., Cui, M., Jiang, B., Chen, Y., Tang, J., Song, J., Peng,  
666 P., Zhang, G.: Molecular compositions and optical properties of dissolved brown carbon in biomass burning,  
667 coal combustion, and vehicle emission aerosols illuminated by excitation–emission matrix spectroscopy  
668 and Fourier transform ion cyclotron resonance mass spectrometry analysis. Atmos. Chem. Phys. 20, 2513-  
669 2532. 10.5194/acp-20-2513-2020, 2020.

670 Tao, S., Lu, X., Levac, N., Bateman, A. P., Nguyen, T. B., Bones, D. L., Nizkorodov, S. A., Laskin, J.,  
671 Laskin, A., Yang, X.: Molecular Characterization of Organosulfates in Organic Aerosols from Shanghai and  
672 Los Angeles Urban Areas by Nanospray-Desorption Electrospray Ionization High-Resolution Mass  
673 Spectrometry. Environmental Science & Technology. 48, 10993-11001. 10.1021/es5024674, 2014.

674 Tolocka, M. P., Turpin, B.: Contribution of Organosulfur Compounds to Organic Aerosol Mass.  
675 Environmental Science & Technology. 46, 7978-7983. 10.1021/es300651v, 2012.

676 Wach, P., Spólnik, G., Rudziński, K. J., Skotak, K., Claeys, M., Danikiewicz, W., Szmigielski, R.:  
677 Radical oxidation of methyl vinyl ketone and methacrolein in aqueous droplets: Characterization of  
678 organosulfates and atmospheric implications. Chemosphere. 214, 1-9.  
679 <https://doi.org/10.1016/j.chemosphere.2018.09.026>, 2019.

680 Wang, G., Zhang, R., Gomez, M. E., Yang, L., Levy Zamora, M., Hu, M., Lin, Y., Peng, J., Guo, S.,  
681 Meng, J., Li, J., Cheng, C., Hu, T., Ren, Y., Wang, Y., Gao, J., Cao, J., An, Z., Zhou, W., Li, G., Wang, J.,  
682 Tian, P., Marrero-Ortiz, W., Secrest, J., Du, Z., Zheng, J., Shang, D., Zeng, L., Shao, M., Wang, W., Huang,  
683 Y., Wang, Y., Zhu, Y., Li, Y., Hu, J., Pan, B., Cai, L., Cheng, Y., Ji, Y., Zhang, F., Rosenfeld, D., Liss, P. S.,  
684 Duce, R. A., Kolb, C. E., Molina, M. J.: Persistent sulfate formation from London Fog to Chinese haze.  
685 Proceedings of the National Academy of Sciences. 113, 13630-13635. 10.1073/pnas.1616540113, 2016a.

686 Wang, G., Zhang, R., Gomez, M. E., Yang, L., Levy Zamora, M., Hu, M., Lin, Y., Peng, J., Guo, S.,  
687 Meng, J., Li, J., Cheng, C., Hu, T., Ren, Y., Wang, Y., Gao, J., Cao, J., An, Z., Zhou, W., Li, G., Wang, J.,  
688 Tian, P., Marrero-Ortiz, W., Secrest, J., Du, Z., Zheng, J., Shang, D., Zeng, L., Shao, M., Wang, W., Huang,  
689 Y., Wang, Y., Zhu, Y., Li, Y., Hu, J., Pan, B., Cai, L., Cheng, Y., Ji, Y., Zhang, F., Rosenfeld, D., Liss, P. S.,  
690 Duce, R. A., Kolb, C. E., Molina, M. J.: Persistent sulfate formation from London Fog to Chinese haze.

691 113, 13630-13635. doi:10.1073/pnas.1616540113, 2016b.

692 Wang, H., Ma, X., Tan, Z., Wang, H., Chen, X., Chen, S., Gao, Y., Liu, Y., Liu, Y., Yang, X., Yuan, B.,  
693 Zeng, L., Huang, C., Lu, K., Zhang, Y.: Anthropogenic monoterpenes aggravating ozone pollution. National  
694 Science Review. 9, nwac103. 10.1093/nsr/nwac103, 2022a.

695 Wang, K., Zhang, Y., Huang, R.-J., Wang, M., Ni, H., Kampf, C. J., Cheng, Y., Bilde, M., Glasius, M.,  
696 Hoffmann, T.: Molecular Characterization and Source Identification of Atmospheric Particulate  
697 Organosulfates Using Ultrahigh Resolution Mass Spectrometry. Environmental Science & Technology. 53,  
698 6192-6202. 10.1021/acs.est.9b02628, 2019a.

699 Wang, Y., Ren, J., Huang, X. H. H., Tong, R., Yu, J. Z.: Synthesis of Four Monoterpene-Derived  
700 Organosulfates and Their Quantification in Atmospheric Aerosol Samples. Environmental Science &  
701 Technology. 51, 6791-6801. 10.1021/acs.est.7b01179, 2017.

702 Wang, Y., Hu, M., Guo, S., Wang, Y., Zheng, J., Yang, Y., Zhu, W., Tang, R., Li, X., Liu, Y., Le Breton,  
703 M., Du, Z., Shang, D., Wu, Y., Wu, Z., Song, Y., Lou, S., Hallquist, M., Yu, J.: The secondary formation of  
704 organosulfates under interactions between biogenic emissions and anthropogenic pollutants in summer in  
705 Beijing. Atmospheric Chemistry and Physics. 18, 10693-10713. 10.5194/acp-18-10693-2018, 2018.

706 Wang, Y., Ma, Y., Li, X., Kuang, B. Y., Huang, C., Tong, R., Yu, J. Z.: Monoterpene and Sesquiterpene  
707  $\alpha$ -Hydroxy Organosulfates: Synthesis, MS/MS Characteristics, and Ambient Presence. Environmental  
708 Science & Technology. 53, 12278-12290. 10.1021/acs.est.9b04703, 2019b.

709 Wang, Y., Hu, M., Wang, Y.-C., Li, X., Fang, X., Tang, R., Lu, S., Wu, Y., Guo, S., Wu, Z., Hallquist,  
710 M., Yu, J. Z.: Comparative Study of Particulate Organosulfates in Contrasting Atmospheric Environments:  
711 Field Evidence for the Significant Influence of Anthropogenic Sulfate and NOx. Environmental Science &  
712 Technology Letters. 7, 787-794. 10.1021/acs.estlett.0c00550, 2020.

713 Wang, Y., Zhao, Y., Wang, Y., Yu, J. Z., Shao, J., Liu, P., Zhu, W., Cheng, Z., Li, Z., Yan, N., Xiao, H.:  
714 Organosulfates in atmospheric aerosols in Shanghai, China: seasonal and interannual variability, origin, and  
715 formation mechanisms. Atmos. Chem. Phys. 21, 2959-2980. 10.5194/acp-21-2959-2021, 2021a.

716 Wang, Y., Zhao, Y., Wang, Y., Yu, J. Z., Shao, J., Liu, P., Zhu, W., Cheng, Z., Li, Z., Yan, N., Xiao, H.:  
717 Organosulfates in atmospheric aerosols in Shanghai, China: seasonal and interannual variability, origin, and  
718 formation mechanisms. Atmospheric Chemistry and Physics. 21, 2959-2980. 10.5194/acp-21-2959-2021,  
719 2021b.

720 Wang, Y., Ma, Y., Kuang, B., Lin, P., Liang, Y., Huang, C., Yu, J. Z.: Abundance of organosulfates  
721 derived from biogenic volatile organic compounds: Seasonal and spatial contrasts at four sites in China.  
722 Science of The Total Environment. 806, 151275. <https://doi.org/10.1016/j.scitotenv.2021.151275>, 2022b.

723 Wang, Y., Feng, Z., Yuan, Q., Shang, D., Fang, Y., Guo, S., Wu, Z., Zhang, C., Gao, Y., Yao, X., Gao,  
724 H., Hu, M.: Environmental factors driving the formation of water-soluble organic aerosols: A comparative  
725 study under contrasting atmospheric conditions. Science of The Total Environment. 866, 161364.  
726 <https://doi.org/10.1016/j.scitotenv.2022.161364>, 2023a.

727 Wang, Y., Liang, S., Le Breton, M., Wang, Q. Q., Liu, Q., Ho, C. H., Kuang, B. Y., Wu, C., Hallquist,  
728 M., Tong, R., Yu, J. Z.: Field observations of C2 and C3 organosulfates and insights into their formation

729 mechanisms at a suburban site in Hong Kong. *Science of The Total Environment*. 904, 166851.  
730 <https://doi.org/10.1016/j.scitotenv.2023.166851>, 2023b.

731 Wei, L., Liu, R., Liao, C., Ouyang, S., Wu, Y., Jiang, B., Chen, D., Zhang, T., Guo, Y., Liu, S. C.: An  
732 observation-based analysis of atmospheric oxidation capacity in Guangdong, China. *Atmospheric*  
733 *Environment*. 318, 120260. <https://doi.org/10.1016/j.atmosenv.2023.120260>, 2024.

734 Wu, Z., Wang, Y., Tan, T., Zhu, Y., Li, M., Shang, D., Wang, H., Lu, K., Guo, S., Zeng, L., Zhang, Y.:  
735 Aerosol Liquid Water Driven by Anthropogenic Inorganic Salts: Implying Its Key Role in Haze Formation  
736 over the North China Plain. *Environmental Science & Technology Letters*. 5, 160-166.  
737 10.1021/acs.estlett.8b00021, 2018.

738 Xu, L., Tsona, N. T., Du, L.: Relative Humidity Changes the Role of SO<sub>2</sub> in Biogenic Secondary  
739 Organic Aerosol Formation. *The Journal of Physical Chemistry Letters*. 12, 7365-7372.  
740 10.1021/acs.jpclett.1c01550, 2021a.

741 Xu, L., Yang, Z., Tsona, N. T., Wang, X., George, C., Du, L.: Anthropogenic–Biogenic Interactions at  
742 Night: Enhanced Formation of Secondary Aerosols and Particulate Nitrogen- and Sulfur-Containing  
743 Organics from  $\beta$ -Pinene Oxidation. *Environmental Science & Technology*. 55, 7794-7807.  
744 10.1021/acs.est.0c07879, 2021b.

745 Xu, R., Chen, Y., Ng, S. I. M., Zhang, Z., Gold, A., Turpin, B. J., Ault, A. P., Surratt, J. D., Chan, M.  
746 N.: Formation of Inorganic Sulfate and Volatile Nonsulfated Products from Heterogeneous Hydroxyl  
747 Radical Oxidation of 2-Methyltetrol Sulfate Aerosols: Mechanisms and Atmospheric Implications.  
748 *Environmental Science & Technology Letters*. 11, 968-974. 10.1021/acs.estlett.4c00451, 2024.

749 Yang, T., Xu, Y., Ye, Q., Ma, Y. J., Wang, Y. C., Yu, J. Z., Duan, Y. S., Li, C. X., Xiao, H. W., Li, Z. Y.,  
750 Zhao, Y., Xiao, H. Y.: Spatial and diurnal variations of aerosol organosulfates in summertime Shanghai,  
751 China: potential influence of photochemical processes and anthropogenic sulfate pollution. *Atmos. Chem.*  
752 *Phys.* 23, 13433-13450. 10.5194/acp-23-13433-2023, 2023.

753 Yang, T., Xu, Y., Ma, Y.-J., Wang, Y.-C., Yu, J. Z., Sun, Q.-B., Xiao, H.-W., Xiao, H.-Y., Liu, C.-Q.:  
754 Field Evidence for Constraints of Nearly Dry and Weakly Acidic Aerosol Conditions on the Formation of  
755 Organosulfates. *Environmental Science & Technology Letters*. 11, 981-987. 10.1021/acs.estlett.4c00522,  
756 2024.

757 Yassine, M. M., Harir, M., Dabek-Zlotorzynska, E., Schmitt-Kopplin, P.: Structural characterization  
758 of organic aerosol using Fourier transform ion cyclotron resonance mass spectrometry: Aromaticity  
759 equivalent approach. *Rapid Communications in Mass Spectrometry*. 28, 2445-2454.  
760 <https://doi.org/10.1002/rcm.7038>, 2014.

761 Ye, C., Lu, K., Song, H., Mu, Y., Chen, J., Zhang, Y.: A critical review of sulfate aerosol formation  
762 mechanisms during winter polluted periods. *Journal of Environmental Sciences*. 123, 387-399.  
763 <https://doi.org/10.1016/j.jes.2022.07.011>, 2023.

764 Ye, J., Abbatt, J. P. D., Chan, A. W. H.: Novel pathway of SO<sub>2</sub> oxidation in the atmosphere: reactions  
765 with monoterpane ozonolysis intermediates and secondary organic aerosol. *Atmos. Chem. Phys.* 18, 5549-  
766 5565. 10.5194/acp-18-5549-2018, 2018.

---

767 Zhang, Y., Chen, Y., Lei, Z., Olson, N. E., Riva, M., Koss, A. R., Zhang, Z., Gold, A., Jayne, J. T.,  
768 Worsnop, D. R., Onasch, T. B., Kroll, J. H., Turpin, B. J., Ault, A. P., Surratt, J. D.: Joint Impacts of Acidity  
769 and Viscosity on the Formation of Secondary Organic Aerosol from Isoprene Epoxydiols (IEPOX) in Phase  
770 Separated Particles. *ACS Earth and Space Chemistry*. 3, 2646-2658. 10.1021/acsearthspacechem.9b00209,  
771 2019.

772 Zhang, Z., Jiang, J., Lu, B., Meng, X., Herrmann, H., Chen, J., Li, X.: Attributing Increases in Ozone  
773 to Accelerated Oxidation of Volatile Organic Compounds at Reduced Nitrogen Oxides Concentrations.  
774 *PNAS Nexus*. 1, pgac266. 10.1093/pnasnexus/pgac266, 2022.

775 Zhao, D., Schmitt, S. H., Wang, M., Acir, I. H., Tillmann, R., Tan, Z., Novelli, A., Fuchs, H., Pullinen,  
776 I., Wegener, R., Rohrer, F., Wildt, J., Kiendler-Scharr, A., Wahner, A., Mentel, T. F.: Effects of NO<sub>x</sub> and  
777 SO<sub>2</sub> on the secondary organic aerosol formation from photooxidation of  $\alpha$ -pinene and limonene. *Atmos.*  
778 *Chem. Phys.* 18, 1611-1628. 10.5194/acp-18-1611-2018, 2018.

779 Zheng, B., Zhang, Q., Zhang, Y., He, K. B., Wang, K., Zheng, G. J., Duan, F. K., Ma, Y. L., Kimoto,  
780 T.: Heterogeneous chemistry: a mechanism missing in current models to explain secondary inorganic  
781 aerosol formation during the January 2013 haze episode in North China. *Atmos. Chem. Phys.* 15, 2031-  
782 2049. 10.5194/acp-15-2031-2015, 2015.

783